

# Synthesis and Structural and Magnetic Studies of Diazine-Bridged Complexes of Copper(II) Cyanate. Crystal Structure of Poly[bis(cyanato-*N*)bis( $\mu$ -methylpyrazine)copper(II)]

Tom Otieno, Steven J. Rettig, Robert C. Thompson,\* and James Trotter

Department of Chemistry, University of British Columbia, 2036 Main Mall, Vancouver, BC, Canada V6T 1Z1

Received February 19, 1993\*

Copper(II) cyanate complexes of composition  $\text{CuL}_n(\text{NCO})_2$ , where  $n$  is 1 for  $\text{L} = \text{pyrazine (pyz)}$ , methylpyrazine (mepyz), and pyridazine (pdz) and  $n$  is 2 for  $\text{L} = \text{mepyz}$  and pyridine (py), have been prepared and characterized by vibrational, electronic, and electron spin resonance spectroscopy, differential scanning calorimetry, and magnetic susceptibility studies to cryogenic temperatures. A single-crystal X-ray diffraction study on  $\text{Cu(mepyz)}_2(\text{NCO})_2$  ( $\text{C}_{12}\text{H}_{12}\text{CuN}_6\text{O}_2$ ), the first compound containing methylpyrazine to be characterized in this way, revealed a two-dimensional square lattice polymeric structure. Its crystals are monoclinic,  $P2_1/c$ , with  $a = 10.480(2)$  Å,  $b = 10.720(2)$  Å,  $c = 25.027(1)$  Å,  $\beta = 93.849(9)^\circ$ , and  $Z = 8$ . The structure was solved by the Patterson method and was refined by full-matrix least-squares procedures to  $R = 0.056$  for 4168 reflections with  $I \geq 3\sigma(I)$ . The compound has terminal cyanates and unsymmetrically bridging methylpyrazine ligands and a structure which provides no facile pathway for exchange. It is magnetically dilute as is  $\text{Cu(py)}_2(\text{NCO})_2$ .  $\text{Cu(py)}_2(\text{NCO})_2$  and  $\text{Cu(pdz)}(\text{NCO})_2$  exhibit antiferromagnetic exchange, and the magnetic susceptibilities of these complexes have been successfully analyzed according to a Heisenberg one-dimensional model yielding  $J$  values of  $-1.2$  and  $-44.0$  cm $^{-1}$ , respectively. The exchange in these complexes is judged to be propagated along extended chains formed by bridging diazine ligands. While the magnetic data for  $\text{Cu(mepyz)}(\text{NCO})_2$  could not be fitted successfully to existing magnetic models, they clearly show the presence of antiferromagnetic coupling of a magnitude comparable to that of the pyrazine analogue. In this case it is proposed that exchange is propagated in such a way that the process is complex and does not approximate either simple one-dimensional or two-dimensional behavior.

## Introduction

Earlier studies on the magnetic properties of pyridine and pyrazine complexes of iron(II) cyanate revealed ferromagnetic exchange in  $\text{Fe(py)}_2(\text{NCO})_2$  ( $\text{py} = \text{pyridine}$ )<sup>1</sup> and antiferromagnetic exchange in  $\text{Fe(py)}_2(\text{NCO})_2$  ( $\text{pyz} = 1,4\text{-diazine, pyrazine}$ ).<sup>2</sup> While the molecular structure of neither compound has been determined by single-crystal X-ray diffraction methods, spectroscopic studies support polymeric structures for both compounds in which ions are linked in chains by single nitrogen atom bridges ( $>\text{NCO}$ ). In  $\text{Fe(py)}_2(\text{NCO})_2$  the chains are cross-linked by bridging pyrazine ligands, while in  $\text{Fe(py)}_2(\text{NCO})_2$  the fifth and sixth coordination sites on Fe are occupied by monodentate ligands, leaving the chains in this compound effectively isolated. The ferromagnetism observed for  $\text{Fe(py)}_2(\text{NCO})_2$  was explained by the presence of orthogonal orbital overlap involving the single nitrogen atoms of the bridging cyanate groups.<sup>1</sup> The observation of antiferromagnetic coupling in  $\text{Fe(py)}_2(\text{NCO})_2$  prompted the suggestion of an exchange mechanism for this compound in which ferromagnetic intrachain interactions via the bridging cyanate groups are combined with antiferromagnetic interchain interactions via the bridging pyrazine ligands, resulting in net, strong, antiferromagnetism.<sup>2</sup> In order to examine more fully the nature of low-dimensional magnetic exchange effects in cyanate complexes, particularly those in which other bridging ligands are present in addition to bridging cyanates, we have extended the work to include complexes of copper.

We report here studies on copper(II) cyanate complexes of pyrazine, methylpyrazine (mepyz), and pyridazine (1,2-diazine, pdz):  $\text{Cu(py)}_2(\text{NCO})_2$ ,  $\text{Cu(mepyz)}_2(\text{NCO})_2$ ,  $\text{Cu(mepyz)}(\text{NCO})_2$ , and  $\text{Cu(pdz)}(\text{NCO})_2$ . For comparison purposes, studies

on the related and previously reported<sup>3</sup> pyridine complex  $\text{Cu(py)}_2(\text{NCO})_2$  are also described.  $\text{Cu(mepyz)}_2(\text{NCO})_2$  was obtained in crystalline form suitable for single-crystal X-ray diffraction studies, the results of which are described here. The X-ray-determined structure of  $\text{Cu(py)}_2(\text{NCO})_2$  was reported earlier by Valach *et al.*<sup>4</sup> For the remainder of the complexes, we have had to rely on indirect methods for structural elucidation, as in the previous studies on the iron(II) complexes.<sup>1,2</sup>

## Experimental Section

**Preparation of the Complexes.** All chemicals were of at least reagent grade quality and were obtained from commercial sources. All compounds described here were sufficiently air-stable that manipulations could be carried out in the atmosphere. Samples were, however, stored in a desiccator over Drierite. The pyridine complex was prepared by a slight modification of a literature procedure.<sup>3</sup> The pyrazine, methylpyrazine, and pyridazine complexes were prepared by two general methods. In method A an aqueous solution (5 mL) of KNCO was added to  $\text{CuSO}_4 \cdot 5\text{H}_2\text{O}$  dissolved in water (5 mL), and the resulting solution was filtered directly into a flask containing an excess (ligand:metal  $\approx 4$ ) of pure ligand (methylpyrazine and pyridazine) or of ligand dissolved in 5 mL of water (pyrazine). In method B lower ligand to metal ratios were used (ratio  $\approx 1$ ) and the ligand or ligand solution was added to the metal solution. In all cases precipitates formed immediately. The mixtures were stirred for 0.5–1 h; then the products were isolated by filtration, washed with water, methanol, and, in some cases, diethyl ether, and finally dried *in vacuo*.

**Bis(pyridine)copper(II) Cyanate,  $\text{Cu(py)}_2(\text{NCO})_2$ .** This blue compound was prepared as described in the literature<sup>3</sup> with the amounts of reagents scaled down by a factor of 4 in the present work. Yield: 74%. Anal. Calcd for  $\text{CuC}_{12}\text{H}_{10}\text{N}_4\text{O}_2$ : C, 47.14; H, 3.30; N, 18.32. Found: 47.14; H, 3.30; N, 18.36.

**(Pyrazine)copper(II) Cyanate,  $\text{Cu(py)}_2(\text{NCO})_2$ .** This compound was prepared by method A using 8.53 mmol of KNCO, 4.05 mmol of  $\text{CuSO}_4 \cdot 5\text{H}_2\text{O}$ , and 16.4 mmol of pyrazine. The blue product was washed

\* Abstract published in *Advance ACS Abstracts*, September 1, 1993.

(1) Little, B. F.; Long, G. J. *Inorg. Chem.* **1978**, *17*, 3401.  
(2) Haynes, J. S.; Kostikas, A.; Sams, J. R.; Simopoulos, A.; Thompson, R. C. *Inorg. Chem.* **1987**, *26*, 2630.

(3) Burmeister, J. L.; O'Sullivan, T. P. *Inorg. Chim. Acta* **1969**, *3*, 479.

(4) Valach, F.; Dunaj-Jurco, M.; Handlovic, M. *J. Cryst. Mol. Struct.* **1980**, *10*, 61.

Table I. Crystallographic Data for  $\text{Cu}(\text{mepyz})_2(\text{NCO})_2^{a,b}$ 

formula	$\text{C}_{12}\text{H}_{12}\text{CuN}_6\text{O}_2$
fw	335.81
crystal system	monoclinic
space group	$P2_1/c$ (No. 14)
$a$ , Å	10.480(2)
$b$ , Å	10.720(2)
$c$ , Å	25.027(1)
$\beta$ , deg	93.849(9)
$Z$	8
$V$ , Å <sup>3</sup>	2805.4(8)
$\rho_{\text{calcd}}$ , g cm <sup>-3</sup>	1.590
$F(000)$	1368
$\mu$ , cm <sup>-1</sup>	22.92
radiation ( $\lambda$ , Å)	Cu K $\alpha$ (1.541 78)
$T$ , °C	21
$R$	0.056
$R_w$	0.066

<sup>a</sup> Estimated standard deviations in the last digit are given in parentheses.

<sup>b</sup>  $R = \sum ||F_o| - |F_c|| / \sum |F_o|$  and  $R_w = (\sum w(|F_o| - |F_c|)^2 / \sum w|F_o|^2)^{1/2}$  where  $w = 4F_o^2 / \sigma^2(F_o^2)$ .

with water and methanol and then dried for 2 h at room temperature and for 5 h at 80 °C. Yield: 57%. Anal. Calcd for  $\text{CuC}_6\text{H}_4\text{N}_4\text{O}_2$ : C, 31.66; H, 1.77; N, 24.61. Found: C, 31.48; H, 1.80; N, 24.75.

(Pyridazine)copper(II) Cyanate,  $\text{Cu}(\text{pdz})(\text{NCO})_2$ . Method A was employed using 8.30 mmol of KNCO, 4.01 mmol of  $\text{CuSO}_4 \cdot 5\text{H}_2\text{O}$ , and 14 mmol of pyridazine. The blue product was washed with water, methanol, and finally diethyl ether. Drying was done at room temperature for 5 h. Yield: 66%. Anal. Calcd for  $\text{CuC}_6\text{H}_4\text{N}_4\text{O}_2$ : C, 31.66; H, 1.77; N, 24.61. Found: C, 31.53; H, 1.82; N, 24.44.

Poly[bis(cyanato-*N*)bis( $\mu$ -methylpyrazine)copper(II)],  $\text{Cu}(\text{mepyz})_2(\text{NCO})_2$ . Method A was initially followed using 8.46 mmol of KNCO, 4.01 mmol of  $\text{CuSO}_4 \cdot 5\text{H}_2\text{O}$ , and 16 mmol of methylpyrazine. The initial product was washed with water and then methanol (both containing a few drops of mepyz) and dried at room temperature. Methylpyrazine (10 mL) was added to this material, and the mixture was stirred for 2 h and then filtered. The filtrate yielded blue crystals in the form of very thin sheets. The yield after  $\approx 1$  week and decanting and washing with diethyl ether was 24%. Anal. Calcd for  $\text{CuC}_{12}\text{H}_{12}\text{N}_6\text{O}_2$ : C, 42.92; H, 3.60; N, 25.03. Found: C, 42.76; H, 3.59; N, 25.19.

(Methylpyrazine)copper(II) Cyanate,  $\text{Cu}(\text{mepyz})(\text{NCO})_2$ . This compound was prepared by method B using 8.42 mmol of KNCO, 4.01 mmol of  $\text{CuSO}_4 \cdot 5\text{H}_2\text{O}$ , and 4.3 mmol of methylpyrazine. The water and methanol used for washing the product both contained a few drops of methylpyrazine. Drying was done for 0.25 h at room temperature. The yield of the blue product was 71%. Anal. Calcd for  $\text{CuC}_7\text{H}_6\text{N}_4\text{O}_2$ : C, 34.79; H, 2.50; N, 23.18. Found: C, 34.93; H, 2.65; N, 22.99.

X-ray Crystallographic Analysis of  $\text{Cu}(\text{mepyz})_2(\text{NCO})_2$ . Crystallographic data appear in Table I. The crystals are unstable and decompose rapidly. The specimen employed for data collection was taken directly from a freshly prepared solution and was mounted wet in a capillary tube. The final unit-cell parameters were obtained by least-squares calculations on the setting angles for 25 reflections with  $2\theta = 106.1\text{--}114.8^\circ$ . The intensities of three standard reflections, measured every 200 reflections throughout the data collection, showed only small random fluctuations. The data were processed<sup>5</sup> and corrected for Lorentz and polarization effects and absorption (empirical, based on azimuthal scans for three reflections).

The structure was solved by conventional heavy-atom methods, the coordinates of the Cu atoms being determined from the Patterson function and those of the remaining non-hydrogen atoms from subsequent difference Fourier syntheses. There are two crystallographically independent molecules in the asymmetric unit. The two independent formula units are related by a pseudo-*C*-centering relationship which is broken by the orientation of the mepyz ligands. Reflections with  $h + k$  odd are, on average, about half as intense as those with  $h + k$  even. All non-hydrogen atoms were refined with anisotropic thermal parameters. The hydrogen atoms were fixed in calculated positions ( $\text{C-H} = 0.98$  Å,  $B(\text{H}) = 1.2B(\text{bonded atom})$ ). A secondary extinction correction was applied, the final value of the extinction coefficient being  $1.03(6) \times 10^{-6}$ . The crystal used for data collection was twinned, the reflections from the twin components overlapping for reflections with  $h = 3n$ . As a result, the

Table II. Final Atomic Coordinates (Fractional) and  $B_{\text{eq}}$  Values (Å<sup>2</sup>)<sup>a</sup>

atom	$x$	$y$	$z$	$B_{\text{eq}}$
Cu(1)	0.01986(7)	0.17501(6)	0.14276(3)	3.52(3)
O(1)	0.1038(4)	0.1120(4)	-0.0147(1)	5.1(2)
O(2)	-0.0172(5)	0.1444(6)	0.3085(2)	9.2(3)
N(1)	-0.1053(4)	0.3257(3)	0.1406(1)	3.2(2)
N(2)	-0.2794(4)	0.5227(4)	0.1364(2)	3.7(2)
N(3)	0.1364(3)	0.0193(3)	0.1463(1)	3.2(1)
N(4)	0.3030(4)	-0.1824(4)	0.1460(2)	3.6(2)
N(5)	0.0249(4)	0.1820(4)	0.0660(2)	3.8(2)
N(6)	0.0313(4)	0.1825(4)	0.2204(2)	4.6(2)
C(1)	-0.1048(4)	0.4137(4)	0.1029(2)	3.6(2)
C(2)	-0.1922(4)	0.5119(4)	0.1006(2)	3.5(2)
C(3)	-0.2797(5)	0.4319(5)	0.1731(2)	4.2(2)
C(4)	-0.1947(5)	0.3355(5)	0.1766(2)	4.0(2)
C(5)	-0.1886(5)	0.6090(6)	0.0574(2)	5.2(3)
C(6)	0.1145(4)	-0.0775(4)	0.1138(2)	3.2(2)
C(7)	0.1955(4)	-0.1802(4)	0.1136(2)	3.4(2)
C(8)	0.3238(5)	-0.0866(5)	0.1789(2)	3.8(2)
C(9)	0.2411(5)	0.0133(4)	0.1800(2)	3.6(2)
C(10)	0.1626(5)	-0.2883(5)	0.0773(2)	4.4(2)
C(11)	0.0645(5)	0.1460(4)	0.0263(2)	3.5(2)
C(12)	0.0055(5)	0.1619(5)	0.2633(2)	4.4(2)
Cu(2)	0.52126(7)	0.67233(6)	0.14248(3)	3.54(3)
O(3)	0.3920(4)	0.6140(4)	-0.0159(1)	5.4(2)
O(4)	0.4509(5)	0.6674(6)	0.3035(2)	9.1(3)
N(7)	0.6433(4)	0.8260(3)	0.1423(1)	3.3(2)
N(8)	0.8189(4)	1.0211(4)	0.1392(2)	3.4(2)
N(9)	0.4027(3)	0.5184(4)	0.1444(1)	3.3(2)
N(10)	0.2389(4)	0.3138(4)	0.1441(2)	3.5(2)
N(11)	0.4928(4)	0.6831(4)	0.0656(2)	3.8(2)
N(12)	0.5400(4)	0.6710(4)	0.2202(2)	4.4(2)
C(13)	0.6342(4)	0.9116(4)	0.1040(2)	3.5(2)
C(14)	0.7215(4)	1.0105(4)	0.1018(2)	3.4(2)
C(15)	0.8271(5)	0.9324(5)	0.1766(2)	3.9(2)
C(16)	0.7414(5)	0.8364(5)	0.1792(2)	3.7(2)
C(17)	0.7064(5)	1.1054(5)	0.0583(2)	5.0(3)
C(18)	0.4173(4)	0.4198(4)	0.1132(2)	3.3(2)
C(19)	0.3380(4)	0.3159(4)	0.1128(2)	3.5(2)
C(20)	0.2239(5)	0.4132(5)	0.1754(2)	3.7(2)
C(21)	0.3046(4)	0.5134(4)	0.1760(2)	3.6(2)
C(22)	0.3630(5)	0.2062(5)	0.0781(2)	4.6(2)
C(23)	0.4440(5)	0.6476(4)	0.0258(2)	3.5(2)
C(24)	0.4942(5)	0.6703(6)	0.2605(2)	4.5(3)

$$^a B_{\text{eq}} = (8/3)\pi^2 \sum U_{ij} a_i^* a_j^* (\mathbf{a}_i \cdot \mathbf{a}_j)$$

observed intensities for some planes (especially those having  $h = 3$ ) were larger than the calculated values. In the final stages of refinement about 50 such reflections were removed from the calculations. It should be noted that there was no evidence for the presence of disordered solvent in the lattice. Neutral-atom scattering factors for all atoms and an anomalous dispersion corrections for the non-hydrogen atoms were taken from ref 6. Final atomic coordinates, equivalent isotropic thermal parameters, and selected bond lengths and bond angles appear in Tables II and III. Complete tables of crystallographic data, hydrogen atom parameters, anisotropic thermal parameters, torsion angles, intermolecular contacts, and least-squares planes are included as supplementary material.

Physical Measurements. Differential scanning calorimetry (DSC) studies in the 35–450 °C temperature range were made using equipment and procedures previously described<sup>7</sup> with the only difference being that the measuring cell atmosphere was, instead of air, nitrogen gas at a flow rate of 50 mL min<sup>-1</sup>. Infrared spectra in the range 4000–250 cm<sup>-1</sup> were recorded on a Perkin-Elmer Model 598 spectrometer using samples milled in Nujol or hexachlorobutadiene and pressed between KRS-5 plates (Harshaw Chemical Co.). Calibration was achieved using polystyrene, and band frequencies are considered accurate to  $\pm 3$  cm<sup>-1</sup>. Electronic spectra in the 25 000–5000 cm<sup>-1</sup> range were recorded on a Cary 5 UV-vis-near-IR spectrophotometer. Samples were milled in Nujol and sandwiched between quartz glass plates. A second set of plates containing only Nujol was placed in the reference beam. EPR spectra of powder

(6) *International Tables for X-Ray Crystallography*; Kynoch Press: Birmingham, U.K. (present distributor Kluwer Academic Publishers, Dordrecht, The Netherlands), 1974; Vol. IV, pp 99–102 and 149.

(7) Haynes, J. S.; Oliver, K. W.; Thompson, R. C. *Can. J. Chem.* **1985**, *63*, 1111.

(5) TEXSAN/TEXRAY structure analysis package (Molecular Structure Corp., 1985).

**Table III.** Selected Bonding Parameters for  $\text{Cu}(\text{mepyz})_2(\text{NCO})_2$  (Distances, Å; Angles, deg)

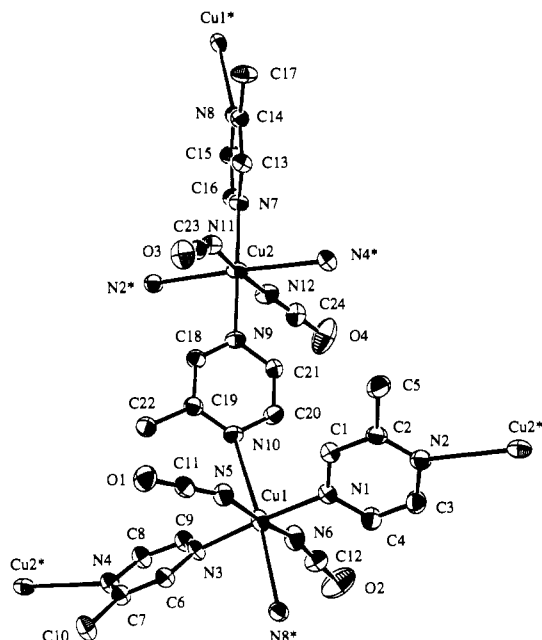
Coordination Sphere of the Copper Ion			
Cu(1)–N(1)	2.080(4)	Cu(1)–N(6)	1.939(4)
Cu(1)–N(3)	2.067(4)	Cu(1)–N(8) <sup>c</sup>	2.672(4)
Cu(1)–N(5)	1.927(4)	Cu(1)–N(10)	2.734(4)
N(1)–Cu(1)–N(3)	176.9(2)	N(3)–Cu(1)–N(8) <sup>c</sup>	88.0(1)
N(5)–Cu(1)–N(6)	173.1(2)	N(3)–Cu(1)–N(10)	86.9(1)
N(8) <sup>c</sup> –Cu(1)–N(10)	174.7(1)	N(5)–Cu(1)–N(8) <sup>c</sup>	93.7(2)
N(1)–Cu(1)–N(5)	90.2(2)	N(5)–Cu(1)–N(10)	85.0(2)
N(1)–Cu(1)–N(6)	89.4(2)	N(6)–Cu(1)–N(8) <sup>c</sup>	93.2(2)
N(1)–Cu(1)–N(8) <sup>c</sup>	89.1(1)	N(6)–Cu(1)–N(10)	88.2(2)
N(1)–Cu(1)–N(10)	96.0(1)	Cu(1)–N(5)–C(11)	150.5(4)
N(3)–Cu(1)–N(5)	91.1(2)	Cu(1)–N(6)–C(12)	158.0(5)
N(3)–Cu(1)–N(6)	89.6(2)		
NCO			
O(1)–C(11)	1.190(6)	N(5)–C(11)	1.167(6)
O(2)–C(12)	1.186(6)	N(6)–C(12)	1.147(6)
O(1)–C(11)–N(5)	178.3(6)	O(2)–C(12)–N(6)	177.0(7)
mepyz <sup>b</sup>			
N–CH	1.335(6)	C–CH	1.370(7)
N–CCH3	1.338(6)	C–CCH3	1.394(6)
C–N–C	116.6(4)	N–C–C	121.7(4)

<sup>a</sup> Estimated standard deviations in the least significant figure are given in parentheses. <sup>b</sup> Mean values. Pertinent data pertaining to the Cu(2) chromophore were included in the calculation of mean values presented in the table and text. <sup>c</sup> Symmetry operation  $x - 1, y - 1, z$ .

samples at  $\approx 90$  K were recorded using previously described equipment.<sup>8</sup> X-ray powder diffraction patterns of samples milled in *n*-octane and smeared on glass plates were recorded in the range  $2\theta = 5$ – $60^\circ$  using a Rigaku Rotaflex rotating-anode X-ray powder diffractometer (Ni-filtered  $\text{Cu K}\alpha$  radiation). Magnetic susceptibilities over the temperature range  $\approx 4.2$ – $82$  K were measured at an applied field of 9225 Oe using a PAR Model 155 vibrating-sample magnetometer as previously described.<sup>9</sup> Samples were held in Kel-F capsules. Susceptibility measurements revealed that none of the samples showed field-dependent susceptibilities between 9225 and 7501 Oe. Magnetic susceptibilities for  $\text{Cu}(\text{py})_2(\text{NCO})_2$  at high temperatures (86–292 K) were measured using a Gouy balance described earlier.<sup>10</sup> This instrument has since been equipped with a Mettler AE 163 balance. For  $\text{Cu}(\text{pdz})(\text{NCO})_2$ , magnetic susceptibilities over the range 5–300 K and at a field of 10 000 Oe were measured using a Quantum Design (MPMS) SQUID magnetometer. The sample holder, possessing a constant cross-sectional area, was made from PVC. Magnetic susceptibilities were corrected for diamagnetism of all atoms (copper, –11; pyridine, –49; pyrazine, –45; methylpyrazine, –57; pyridazine, –45; cyanate, –21) and temperature-independent paramagnetism of copper, 60. All corrections are in units of  $10^{-6} \text{ cm}^3 \text{ mol}^{-1}$ . Carbon, hydrogen, and nitrogen analyses were performed by P. Borda of this department.

## Results

**Structure of  $\text{Cu}(\text{mepyz})_2(\text{NCO})_2$ .** The coordination geometry about copper and the atom-numbering scheme in  $\text{Cu}(\text{mepyz})_2(\text{NCO})_2$  are shown in Figure 1. The extended two-dimensional polymeric structure of this compound is depicted in Figure 2. The unit cell parameters, final atom coordinates (non-hydrogen), equivalent isotropic thermal parameters, and selected bonding parameters are given in Tables I–III. The structure of  $\text{Cu}(\text{mepyz})_2(\text{NCO})_2$  consists of parallel sheets each comprising an infinite square array of copper ions bridged by bidentate methylpyrazine ligands. Coordination number 6 for each copper ion is completed by *trans* cyanato-*N* groups. The sheets are

**Figure 1.** View of the coordination geometry about copper in  $\text{Cu}(\text{mepyz})_2(\text{NCO})_2$  with the atom-numbering scheme.**Table IV.** Selected Spectral Data for Copper(II) Cyanate Complexes<sup>a,b</sup>

	1	2	3	4	5
Infrared					
$\nu_{\text{CN}}$	2155 sh	2167 sh	2180 vs, br	2143 w	2148 sh
	2253 vs, br	2221 vs, br	2180 vs, br	2223 vs, br	2204 vs, br
$\nu_{\text{CO}}$	1354 w	1348 w	1352 m	1353 w	1327 s
$\delta_{\text{NCO}}$	615 s	614 s	613 s	615 s	614 s
	632 s	628 m	646 m, br	638 m	626 s
$\text{py}^c$					440 s
					642 m
					1602 s
$\text{pyz}^d$	494 s				
$\text{mepyz}^e$		436 s	439 } m, sp		
		507 s	448 }		
			522 m		
Electronic					
max	16 600	13 400	16 200	15 600	16 600
sh	$\approx 13 700$	$\approx 16 100$	$\approx 14 600$	<i>f</i>	$\approx 13 800$
EPR <sup>f</sup>					
$g_1$	2.288	2.212	2.280		
$g_2$	2.077	2.150	2.079		
$g_3$		2.057			
$g_0$	2.147	2.140	2.146	2.094	2.180

<sup>a</sup> All infrared and electronic spectral data are in  $\text{cm}^{-1}$ . s = strong, m = medium, w = weak, v = very, sh = shoulder, sp = split, br = broad. <sup>b</sup> 1 =  $\text{Cu}(\text{pyz})(\text{NCO})_2$ , 2 =  $\text{Cu}(\text{mepyz})_2(\text{NCO})_2$ , 3 =  $\text{Cu}(\text{mepyz})(\text{NCO})_2$ , 4 =  $\text{Cu}(\text{pdz})(\text{NCO})_2$ , 5 =  $\text{Cu}(\text{py})_2(\text{NCO})_2$ . <sup>c</sup> Correspond to free-ligand bands<sup>18</sup> at 405, 605, and  $1583 \text{ cm}^{-1}$ . <sup>d</sup> Correspond to free-ligand band<sup>20</sup> at  $417 \text{ cm}^{-1}$ . <sup>e</sup> Correspond to free-ligand bands (this work) at 410 and  $472 \text{ cm}^{-1}$ . <sup>f</sup> Shoulder not observed, but band is very broad and asymmetric. <sup>g</sup> Error in *g* values:  $\pm 0.003$ . When only two *g* values are observed,  $g_1 = g_{\parallel}$  and  $g_2 = g_{\perp}$ .  $g_0$  = isotropic *g* value. For orthorhombic and axial systems,  $g_0 = (g_1 + g_2 + g_3)/3$  and  $g_0$  and  $(g_1 + 2g_{\perp})/3$ , respectively.

disposed such that the copper ions in one sheet lie vertically above and below the centers of the squares formed by the copper ions of adjacent sheets.

**Thermal, Spectral, X-ray Powder Diffraction, and Magnetic Data.** The DSC thermogram of  $\text{Cu}(\text{mepyz})_2(\text{NCO})_2$  reveals an endothermic peak at  $145^\circ\text{C}$  and three exothermic events at about 160, 190, and  $290^\circ\text{C}$ . The thermogram of  $\text{Cu}(\text{mepyz})(\text{NCO})_2$  is the same as above except that the endothermic event is missing.  $\text{Cu}(\text{pyz})(\text{NCO})_2$ ,  $\text{Cu}(\text{pdz})(\text{NCO})_2$ , and  $\text{Cu}(\text{py})_2(\text{NCO})_2$  show no events prior to exothermic decomposition at 140, 115, and  $135^\circ\text{C}$ , respectively.

- (8) Herring, F. G.; Hwang, G.; Lee, K. C.; Mistry, F.; Phillips, P. S.; Willner, H.; Aubke, F. *J. Am. Chem. Soc.* **1992**, *114*, 1271.  
 (9) Haynes, J. S.; Oliver, K. W.; Rettig, S. J.; Thompson, R. C.; Trotter, J. *Can. J. Chem.* **1984**, *62*, 891.  
 (10) Clark, H. C.; O'Brien, R. J. *Can. J. Chem.* **1961**, *39*, 1030.

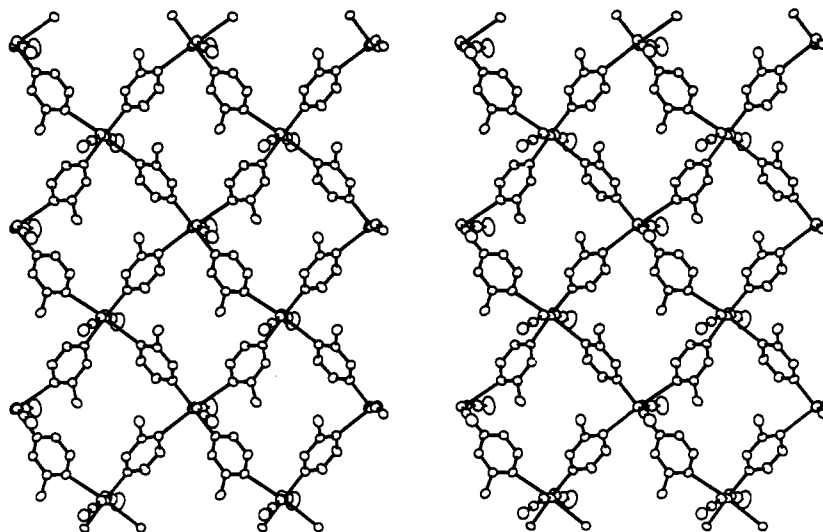


Figure 2. Stereoview of the extended two-dimensional structure of  $\text{Cu}(\text{mepyz})_2(\text{NCO})_2$ .

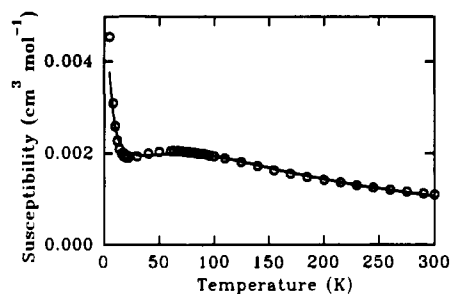


Figure 3. Magnetic susceptibility versus temperature plot for  $\text{Cu}(\text{pdz})(\text{NCO})_2$ . The line was generated using the linear-chain model with  $J = -44.0 \text{ cm}^{-1}$ ,  $\%P = 3.02$ , and  $g = 2.09$ .

Selected infrared frequencies for the five complexes are given in Table IV. The complexes exhibit single, broad, asymmetric absorption bands in their electronic spectra ( $25\,000\text{--}5000 \text{ cm}^{-1}$  range), and the positions of the band maxima are listed in Table IV. The EPR spectrum of  $\text{Cu}(\text{pdz})(\text{NCO})_2$  consists of a single, broad, somewhat asymmetric signal, while the spectra of  $\text{Cu}(\text{pyz})(\text{NCO})_2$  and  $\text{Cu}(\text{mepyz})(\text{NCO})_2$  indicate axial symmetry and that of  $\text{Cu}(\text{mepyz})_2(\text{NCO})_2$  indicates rhombic symmetry. The nearly isotropic EPR spectrum was observed for  $\text{Cu}(\text{py})_2(\text{NCO})_2$ , consistent with an earlier study.<sup>11</sup> The derived  $g$  values for the complexes are given in Table IV.

Data from X-ray powder diffraction studies have been deposited as supplementary material. They show that  $\text{Cu}(\text{pyz})(\text{NCO})_2$  is isomorphous with its nickel analogue<sup>12</sup> but not with  $\text{Cu}(\text{pdz})(\text{NCO})_2$  or  $\text{Cu}(\text{mepyz})(\text{NCO})_2$ .

$\text{Cu}(\text{mepyz})_2(\text{NCO})_2$  and  $\text{Cu}(\text{py})_2(\text{NCO})_2$  exhibit temperature-independent magnetic moments of  $1.84 \mu_B$  (82–2.4 K) and  $1.81 \mu_B$  (292–2.5 K), respectively. A temperature dependence is seen for the moments of  $\text{Cu}(\text{pyz})(\text{NCO})_2$  and  $\text{Cu}(\text{mepyz})(\text{NCO})_2$ . The magnetic moment of the former decreases from 1.79 to  $1.16 \mu_B$ , and that of the latter, from 1.71 to  $1.10 \mu_B$ , between 81 and  $\approx 2.3 \text{ K}$ .  $\text{Cu}(\text{pdz})(\text{NCO})_2$  has a strongly temperature-dependent magnetic moment, ranging from  $1.63 \mu_B$  at 300 K to  $0.43 \mu_B$  at 5 K. Its magnetic susceptibility, plotted as a function of temperature in Figure 3, shows a broad maximum at  $\approx 65 \text{ K}$ . Magnetic susceptibility versus temperature data are deposited as supplementary material for all complexes.

## Discussion

**Thermal Properties.** The DSC studies on  $\text{Cu}(\text{mepyz})_2(\text{NCO})_2$  and  $\text{Cu}(\text{mepyz})(\text{NCO})_2$  show that the former complex loses 1

mol of methylpyrazine at  $145 \text{ }^\circ\text{C}$  in a single endothermic step to yield the mono(methylpyrazine) derivative. Subsequent thermal decomposition of the latter species appears to take place in at least three distinct exothermic steps. This contrasts with the observations made on the mono(pyrazine) and -(pyridazine) complexes, each of which appear to thermally decompose in a single exothermic step. Other researchers have reported  $\text{Cu}(\text{py})_2(\text{NCO})_2$  to decompose at  $113 \text{ }^\circ\text{C}$ ,<sup>3</sup> whereas we find the decomposition temperature to be  $135 \text{ }^\circ\text{C}$  for this compound. No details were given in the earlier study on how the decomposition temperature was determined, and we are unable to explain the discrepancy between the two studies.

**Infrared Spectra.** Previous studies of cyanate complexes have shown that useful information on the mode of coordination of the cyanate ion may be obtained from an examination of infrared spectra.<sup>13–16</sup> The three normal modes of vibration of the linear  $\text{NCO}^-$  anion are antisymmetric stretching  $\nu_1$  ( $\nu_{\text{CN}}$ ), bending  $\nu_2$  ( $\delta_{\text{NCO}}$ ), and pseudosymmetric stretching  $\nu_3$  ( $\nu_{\text{CO}}$ ). In the spectrum of the free ion,<sup>17</sup>  $\nu_{\text{CN}}$  occurs at  $2165 \text{ cm}^{-1}$  and  $\delta_{\text{NCO}}$  vibrations occur at  $628$  and  $637 \text{ cm}^{-1}$ . A doublet, due to Fermi resonance between  $\nu_{\text{CO}}$  and the first overtone of  $\delta_{\text{NCO}}$ , is observed at  $1302$  and  $1207 \text{ cm}^{-1}$ . The unperturbed  $\nu_{\text{CO}}$  is calculated to occur at  $1254 \text{ cm}^{-1}$ .

In the complexes studied here  $\nu_{\text{CO}}$  is observed at higher frequencies than the free-ion value, and on the basis of earlier studies involving cyanate complexes,<sup>15,16</sup> this is consistent with N-bonding rather than O-bonding. N-bonding for the cyanates is confirmed for  $\text{Cu}(\text{mepyz})_2(\text{NCO})_2$  by the X-ray structure reported here, and although the earlier X-ray study on  $\text{Cu}(\text{py})_2(\text{NCO})_2$ <sup>4</sup> revealed cyanates which bridge in an end-to-end fashion, the  $\text{Cu-N}$  and  $\text{Cu-O}$  bond lengths of  $1.946(6)$  and  $2.607(5) \text{ \AA}$ , respectively, reveal very unsymmetrical bridging and clearly much stronger bonding to N than to O. In earlier studies,<sup>13,14</sup> it has been observed that  $\delta_{\text{NCO}}$  is split by at most a few wavenumbers when the cyanate ion is terminal, while it typically shows a splitting of  $30$  to  $50 \text{ cm}^{-1}$  when the ion is bridging. The complexes studied here show splittings in  $\delta_{\text{NCO}}$  ranging from  $12$  to  $33 \text{ cm}^{-1}$ .  $\text{Cu}(\text{mepyz})_2(\text{NCO})_2$  and  $\text{Cu}(\text{py})_2(\text{NCO})_2$ , which are known by X-ray studies to have terminal and highly unsymmetrical bridging cyanates, respectively, have  $\delta_{\text{NCO}}$  splittings on the low end of this range ( $14$  and  $12 \text{ cm}^{-1}$ , respectively), generally consistent with the earlier observations. The splitting of  $\delta_{\text{NCO}}$  by  $33 \text{ cm}^{-1}$  in

(13) Bailey, R. A.; Kozak, S. L.; Michelsen, T. W.; Mills, W. N. *Coord. Chem. Rev.* **1971**, *6*, 407.

(14) Nelson, J.; Nelson, S. M. *J. Chem. Soc. A* **1969**, 1597.

(15) Sabatani, A.; Bertini, I. *Inorg. Chem.* **1965**, *4*, 959.

(16) Forster, D.; Goodgame, D. M. L. *J. Chem. Soc.* **1965**, 1286.

(17) Maki, A.; Decius, J. C. *J. Chem. Phys.* **1959**, *31*, 772.

(11) Morazzoni, F.; Pozzi, A.; Rossi, M.; Scotti, R.; Ravasio, N. *Inorg. Chim. Acta* **1990**, *175*, 277.

(12) Otieno, T. Ph.D. Thesis, University of British Columbia, 1993.

$\text{Cu}(\text{mepyz})(\text{NCO})_2$  is consistent with bridging cyanates in this complex, while the splittings of 17 and 23  $\text{cm}^{-1}$  observed for  $\text{Cu}(\text{pyz})(\text{NCO})_2$  and  $\text{Cu}(\text{pdz})(\text{NCO})_2$ , respectively, suggest the presence of terminal or unsymmetrical bridging cyanates in these complexes.

Bands due to the internal vibrations of the neutral-ligand molecules may also be identified in the infrared spectra, and selected frequencies of this type are listed in Table IV.  $\text{Cu}(\text{py})_2(\text{NCO})_2$  shows only those bands expected for coordinated pyridine, consistent with its known structure. In particular, the expected shifts of the free-ligand bands at 1583, 605, and 405  $\text{cm}^{-1}$  to higher frequencies<sup>18,19</sup> are observed. Previous studies on pyrazine complexes have established that while most pyrazine bands exhibit shifts to higher frequencies on coordination, the most sensitive is the band at 417  $\text{cm}^{-1}$  for the free ligand.<sup>2,20-23</sup> It has also been pointed out that shifts in this band to  $\approx 450 \text{ cm}^{-1}$  usually indicate monodentate coordination, whereas shifts to 470  $\text{cm}^{-1}$  or higher may accompany bidentate coordination.<sup>24</sup>  $\text{Cu}(\text{pyz})(\text{NCO})_2$  shows this band at 494  $\text{cm}^{-1}$ , consistent with bidentate, bridging pyrazine coordination. Supporting this is the observation that while complexes containing monodentate pyrazine typically exhibit bands at frequencies near 1230, 920, and 750  $\text{cm}^{-1}$ , no such bands are observed in the spectrum of this complex.<sup>25</sup>

No satisfactory infrared criteria for establishing the coordination modes of methylpyrazine and pyridazine have been established to date. We note, however, that two methylpyrazine bands, at 410 and 472  $\text{cm}^{-1}$  for the free ligand, are shifted to significantly higher frequencies for the complexes (Table IV). While most pyridazine bands of  $\text{Cu}(\text{pdz})(\text{NCO})_2$  are shifted slightly from the free-ligand values, none appears to be sufficiently coordination sensitive to be of diagnostic value.

**Structures of the Complexes.** As determined here by single-crystal X-ray diffraction, the structure of  $\text{Cu}(\text{mepyz})_2(\text{NCO})_2$  consists of parallel sheets each composed of an infinite square array of copper ions bridged by bidentate methylpyrazine ligands. Coordination number 6 for each copper ion is completed by *trans* cyanato-*N* groups (Figure 1). This type of structure has been observed in the bis(pyrazine) complexes  $\text{Fe}(\text{pyz})_2(\text{NCS})_2$ ,<sup>26</sup>  $\text{Cu}(\text{pyz})_2(\text{CH}_3\text{SO}_3)_2$ ,<sup>21</sup>  $\text{Cu}(\text{pyz})_2(\text{ClO}_4)_2$ ,<sup>27</sup> and  $\text{Co}(\text{pyz})_2\text{Cl}_2$ .<sup>28</sup> As a consequence of steric constraints imposed by the methyl substituent, however,  $\text{Cu}(\text{mepyz})_2(\text{NCO})_2$  possesses some unique structural features not observed in the other sheet polymers: (i) the methylpyrazine bridges are unsymmetrical, i.e.  $\text{Cu}\cdots\text{mepyz}-\text{Cu}$ ; (ii) the  $\text{Cu}\cdots\text{mepyz}-\text{Cu}$  chains are slightly bent in a zigzag manner, the turning point being, by extrapolation, at the center of the methylpyrazine rings; (iii) the molecular axes of adjacent copper ions are misaligned by about 75°; (iv) planes of alternate methylpyrazine ligands along any  $\text{Cu}\cdots\text{mepyz}-\text{Cu}$  chain are tilted away from the plane of the copper ions in opposite directions by 30–50°. The dihedral angle between the planes of any two *trans* methylpyrazine groups is about 80°.

Each copper ion in  $\text{Cu}(\text{mepyz})_2(\text{NCO})_2$  is coordinated to four methylpyrazine ligands, two through the nitrogen atoms meta to the methyl substituent and two through the ortho ones. The two remaining coordination sites are occupied by nitrogen atoms of the cyanate groups. The complex has an elongated rhombic-octahedral  $\text{CuN}_2\text{N}'_2\text{N}''_2$  chromophore. The mean Cu–N bond length involving the cyanate groups is 1.935 Å, while that involving the sterically unhindered methylpyrazine nitrogen atoms is 2.076 Å. The sterically hindered nitrogen atoms from the remaining methylpyrazine groups are considerably further from the copper ion (mean Cu–N distance is 2.707 Å). The Cu–N(mepyz) distances may be compared to those in  $\text{Cu}(\text{pyz})_2(\text{CH}_3\text{SO}_3)_2$ , which has strongly bound, equatorially coordinated and weakly bound, axially coordinated pyrazine ligands with Cu–N distances of 2.058(2) and 2.692(2) Å, respectively.<sup>21</sup> Deviations from linearity (*trans* N–Cu–N angles, 173.1–178.6°) and orthogonality (*cis* N–Cu–N angles, 85.0–96.0°) are observed in the bond angles of the coordination polyhedron of copper. This is a further consequence of the steric influence of the methyl groups. Ideal angles were observed in  $\text{Cu}(\text{pyz})_2(\text{ClO}_4)_2$ <sup>27</sup> and, with only two exceptions, in  $\text{Cu}(\text{pyz})_2(\text{CH}_3\text{SO}_3)_2$ .<sup>21</sup>

Even greater deviation from linearity is observed in the Cu–N–C angles of the copper–cyanate fragments which lie in the range 158.0–159.5°. The N–C–O angle, on the other hand, does not depart significantly from linearity, having a mean value of 177.7°. The mean N–C and C–O bond lengths of the NCO group are 1.154(6) and 1.193(6) Å, respectively. Comparable structural features have been observed in other transition metal complexes containing the NCO group.<sup>4,29-31</sup> For instance, in  $\text{Cu}(\text{py})_2(\text{NCO})_2$  the angles Cu–N–C and N–C–O and the distances N–C and C–O are 151.83(61)°, 177.08(86)°, 1.152(10) Å, and 1.182(9) Å, respectively.<sup>4</sup>

The methylpyrazine molecules in  $\text{Cu}(\text{mepyz})_2(\text{NCO})_2$  are all planar within experimental error. This is the first complex containing this ligand whose structure has been determined by X-ray crystallography, and hence, there are no literature values with which the internal bonding parameters can be directly compared.

When the characterization of  $\text{Cu}(\text{py})_2(\text{NCO})_2$  had already been completed in the present work, Morazzoni *et al.*<sup>11</sup> reported that the compound exists in violet and blue forms, designated  $\alpha$  and  $\beta$ , respectively. The color and infrared and ESR spectra of the compound reported here are consistent with its being the  $\beta$  isomer, and it is this isomer that has been structurally characterized by X-ray diffraction.<sup>4</sup> The copper ions in this compound are linked into an infinite three-dimensional lattice by end-to-end bridging cyanate groups. Each copper ion has a distorted  $\text{CuN}_4\text{O}_2$  chromophore composed of two nitrogen atoms from pyridine ligands, two nitrogen atoms from cyanate anions, and two oxygen atoms from a different set of cyanate anions. The "tetragonal" axes of adjacent copper(II) chromophores are approximately orthogonal in this complex.

Proposals for the structures of the remaining three complexes are primarily based on spectral data and on comparisons with structures of analogous complexes. The electronic spectra of all five complexes are similar, but unfortunately, they do not provide unambiguous stereochemical information. They are, nonetheless, typical for tetragonally distorted octahedral copper(II) compounds,<sup>32,33</sup> a stereochemistry confirmed by X-ray studies on  $\text{Cu}(\text{mepyz})_2(\text{NCO})_2$  (this work) and  $\text{Cu}(\text{py})_2(\text{NCO})_2$ .<sup>4</sup>

The infrared spectroscopic data for  $\text{Cu}(\text{pyz})(\text{NCO})_2$  indicate bridging pyrazine ligands with terminal N-bonded or unsymmetrically bridging cyanates. Structures consistent with this

- (18) Wilmshurst, J. K.; Bernstein, H. J. *Can. J. Chem.* **1957**, *35*, 1183.  
 (19) Gill, N. S.; Nuttall, R. H.; Scaife, D. E.; Sharp, D. W. A. *J. Inorg. Nucl. Chem.* **1961**, *18*, 79.  
 (20) Lord, R. C.; Marston, A. L.; Miller, F. A. *Spectrochim. Acta* **1957**, *9*, 113.  
 (21) Haynes, J. S.; Rettig, S. J.; Sams, J. R.; Thompson, R. C.; Trotter, J. *Can. J. Chem.* **1987**, *65*, 420.  
 (22) Haynes, J. S.; Sams, J. R.; Thompson, R. C. *Inorg. Chem.* **1986**, *25*, 3740.  
 (23) Haynes, J. S.; Sams, J. R.; Thompson, R. C. *Can. J. Chem.* **1988**, *66*, 2079.  
 (24) Otieno, T.; Rettig, S. J.; Thompson, R. C.; Trotter, J. *Can. J. Chem.* **1989**, *67*, 1964.  
 (25) Goldstein, M.; Unsworth, W. D. *Spectrochim. Acta* **1971**, *27A*, 1055.  
 (26) Real, J. A.; De Munno, G.; Munoz, M. C.; Julve, M. *Inorg. Chem.* **1991**, *30*, 2701.  
 (27) Darriet, J.; Haddad, M. S.; Duesler, E. N.; Hendrickson, D. N. *Inorg. Chem.* **1979**, *18*, 2679.  
 (28) Carreck, P. W.; Goldstein, M.; McPartlin, E. M.; Unsworth, W. D. *Chem. Commun.* **1971**, 1634.

- (29) Bush, M. A.; Sim, G. A. *J. Chem. Soc. A* **1970**, 605.  
 (30) McPhail, A. T.; Knox, G. R.; Robertson, C. G.; Sim, G. A. *J. Chem. Soc. A* **1971**, 205.  
 (31) Britton, D.; Dunitz, J. D. *Acta Crystallogr.* **1965**, *18*, 424.  
 (32) Lever, A. B. P.; Mantovani, E. *Inorg. Chem.* **1971**, *10*, 817.  
 (33) Morrison, R. M.; Thompson, R. C. *Can. J. Chem.* **1982**, *60*, 1048.

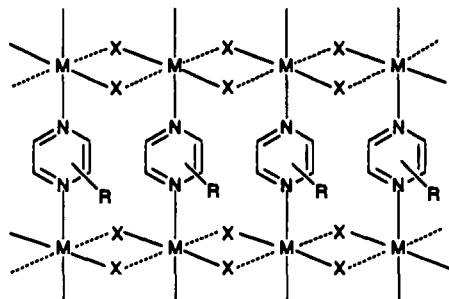


Figure 4. Proposed structures for  $\text{Cu}(\text{pyz})(\text{NCO})_2$  ( $R = \text{H}$ ) and  $\text{Cu}(\text{mepyz})(\text{NCO})_2$  ( $R = \text{CH}_3$ ).  $M = \text{Cu}$ ;  $X = >\text{NCO}$ . The dotted lines illustrate the unsymmetrical nature of the  $>\text{NCO}$  bridges.

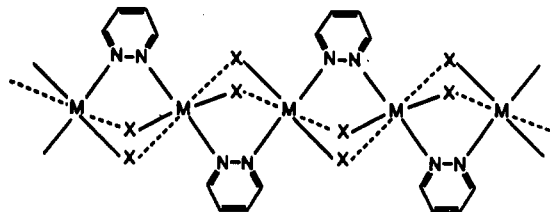


Figure 5. Proposed structure for  $\text{Cu}(\text{pdz})(\text{NCO})_2$ .  $M = \text{Cu}$ ;  $X = >\text{NCO}$ . The dotted lines illustrate the unsymmetrical nature of the  $>\text{NCO}$  bridges.

would include the following: (i) linear chains of copper ions bridged by pyrazine with two terminal cyanates, giving each copper a coordination number of 4; (ii) two-dimensional sheets of copper ions bridged in a square lattice by unsymmetrically end-to-end bridging cyanates ( $-\text{NCO}-$ ), with bridging pyrazine ligands linking the sheets at each copper to give a three-dimensional array; (iii) chains of copper ions linked by unsymmetrical single nitrogen atom cyanate bridges ( $>\text{NCO}$ ), with the chains cross-linked into sheets by pyrazine ligands. We eliminate structure ii as a likely possibility on the basis of the observed EPR spectrum. The complex exhibits a normal axial spectrum ( $g_{\parallel} > g_{\perp} > 2.04$ ; Table IV), indicative of a  $d_{x^2-y^2}$  ground state.<sup>34</sup> This is not consistent with  $-\text{NCO}-$  bridging, since this would produce misaligned tetragonal axes resulting in either a reversed or an isotropic spectrum.<sup>11</sup>  $\text{Cu}(\text{py})_2(\text{NCO})_2$  has the type of  $-\text{NCO}-$  bridging environment in structure ii, and we observe a nearly isotropic spectrum for this compound (Table IV). In structure iii, which is depicted in Figure 4, on the other hand, the tetragonal axes are aligned and a normal axial spectrum is expected. The four-coordinate structure described as i is difficult to definitely eliminate *vis-à-vis* iii, since it represents structure iii in the limit that the long  $\text{Cu}\cdots\text{NCO}$  bonding interactions are insignificant. Nonetheless, evidence against a strictly four-coordinate structure comes from the observation that  $\text{Cu}(\text{pyz})(\text{NCO})_2$  is isomorphous, and most probably isostructural, with its nickel(II) analogue. The latter complex has an electronic spectrum consistent only with a six-coordinate structure.<sup>12</sup> Finally, we note that in an earlier study infrared and Mossbauer data permitted the elimination of possibilities i and ii for the iron analogue,  $\text{Fe}(\text{pyz})(\text{NCO})_2$ , and supported a structure similar to iii but with symmetrically bridging cyanates.<sup>2</sup>

The infrared, EPR, and electronic spectral data for  $\text{Cu}(\text{mepyz})(\text{NCO})_2$  support a structure similar to that proposed for the pyrazine derivative (Figure 4). In this case, however, the  $\delta_{\text{NCO}}$  splitting at  $33\text{ cm}^{-1}$  is significantly greater than that for the pyrazine derivative ( $17\text{ cm}^{-1}$ ), suggesting more symmetrical  $>\text{NCO}$  bridging.

The infrared data obtained for  $\text{Cu}(\text{pdz})(\text{NCO})_2$  support a structure involving terminal or unsymmetrically bridging cyanate ligands. The structure we propose for this complex, Figure 5, involves chains of copper ions joined by pyridazine ligands and unsymmetrically bridging cyanates. In the limit of highly

unsymmetrical cyanate bridges, the structure approaches that of a pyridazine-bridged chain with terminal anionic ligands and four-coordinate copper ions. This latter limiting structure is what is seen in the recently reported X-ray structure determination of the chloride analogue,  $\text{Cu}(\text{pdz})\text{Cl}_2$ .<sup>35</sup> The broad asymmetrical EPR spectrum we observe for the cyanate derivative does not, unfortunately, provide structural information.

**Magnetic Properties.** The magnitude and temperature dependence of the magnetic moment of  $\text{Cu}(\text{mepyz})_2(\text{NCO})_2$  are typical of magnetically dilute copper(II) systems. The absence of significant magnetic exchange coupling in this compound may be ascribed to the unsymmetrical nature of the bridging methylpyrazine ligands and the fact that each copper is effectively isolated from neighboring coppers by long  $\text{Cu}-\text{N}$  bonds. In addition, orbital overlap considerations support lack of exchange as follows. As established by X-ray crystallography, the copper ions in  $\text{Cu}(\text{mepyz})_2(\text{NCO})_2$  have an elongated rhombic-octahedral geometry. The EPR spectrum (Table IV) is consistent with rhombic geometry, and since the lowest  $g$  is greater than 2.04, this in turn is consistent with a  $d_{x^2-y^2}$  ground state.<sup>34</sup> The "tetragonal" axes of all the copper chromophores lie in the same plane. However, the axes on adjacent chromophores are inclined to one another such that a methylpyrazine bridge between two copper centers interacts with a magnetic orbital ( $d_{x^2-y^2}$ ) of one copper ion and a nonmagnetic orbital ( $d_{z^2}$ ) of the second copper ion. Thus there is no continuous path for magnetic exchange between the copper ions in this compound.  $\text{Cu}(\text{py})_2(\text{NCO})_2$  is also magnetically dilute, and this may be explained in a similar manner.

The magnetic behavior of  $\text{Cu}(\text{mepyz})_2(\text{NCO})_2$  may be contrasted with that of the related iron(II) thiocyanate complex  $\text{Fe}(\text{pyz})_2(\text{NCS})_2$ .<sup>26</sup> The two complexes have analogous structures in which six-coordinate metal ions are bridged by neutral ligands in infinite square arrays and anionic ligands are N-bonded in axial positions. In the thiocyanate complex, however, the four equatorial  $\text{Fe}-\text{N}(\text{pyrazine})$  bonds are equal and the tetragonal axes are aligned parallel. In this case measurable antiferromagnetic coupling between metal centers is observed, as the magnetic susceptibility exhibits a maximum at  $8.5\text{ K}$ .<sup>26</sup>

$\text{Cu}(\text{pyz})(\text{NCO})_2$  and  $\text{Cu}(\text{mepyz})(\text{NCO})_2$  exhibit magnetic moments which decrease with decreasing temperature, indicating the presence of antiferromagnetic exchange. The exchange coupling is, however, relatively weak, as evidenced by the fact that no susceptibility maximum is observed over the temperature range studied. According to the proposed structures for these compounds, possible pathways for the exchange involve the bridging neutral ligands and/or the anionic ligands. Accordingly, we examined fits of the susceptibilities to both one-dimensional and two-dimensional Heisenberg models for  $S = 1/2$  systems. The former employs the expressions developed by Hall<sup>36</sup> and Estes *et al.*,<sup>37</sup> and the latter is Lines high-temperature series expansion for a two-dimensional square lattice system.<sup>38</sup> Values of the fitting function,<sup>39</sup>  $F$ , corresponding to the best fit together with the corresponding values of  $g$  and  $J$  are given in Table V.

(35) Fetzer, T.; Lentz, A.; Debaerdemaeker, T.; Abou-El-Wafa, O. Z. *Naturforsch., B* 1990, 45, 199.

(36) Hall, J. W. Ph.D. Thesis, University of North Carolina, 1977.

(37) Estes, W. E.; Hatfield, W. E.; van Ooijen, J. A. C.; Reedijk, J. J. *Chem. Soc., Dalton Trans.* 1980, 2121.

(38) Lines, M. E. *J. Phys. Chem. Solids* 1970, 31, 101.

(39) In the least-squares fitting procedure employed, the following is the function minimized:

$$F = \left[ \frac{1}{n} \sum_{i=1}^n \left( \frac{\chi'_{\text{calc}} - \chi'_{\text{obs}}}{\chi'_{\text{obs}}} \right)^2 \right]^{1/2}$$

where  $n$  is the number of data points and  $\chi'_{\text{obs}}$  and  $\chi'_{\text{calc}}$  are the experimental and calculated molar magnetic susceptibilities. The  $F$  value gives a measure of the quality of the fit between experiment and theory.

**Table V.** Magnetic Parameters for Copper(II) Cyanate Complexes<sup>a</sup>

compd	$-J$ , cm <sup>-1</sup>	$g$	% $P$	$F$
One-dimensional model				
Cu(py <sub>2</sub> z)(NCO) <sub>2</sub> <sup>b</sup>	1.15	2.12	0	0.0105
<i>c</i>	1.22	2.15	0	0.0253
Cu(mepyz)(NCO) <sub>2</sub> <sup>b</sup>	1.17	2.02	0	0.0135
<i>c</i>	1.43	2.15	0	0.0968
Cu(pd <sub>2</sub> z)(NCO) <sub>2</sub> <sup>c</sup>	38.0	2.09	0	0.1631
<i>d</i>	44.0	2.09	3.02	0.0420
Two-Dimensional Model				
Cu(py <sub>2</sub> z)(NCO) <sub>2</sub> <sup>b</sup>	0.70	2.12	0	0.0204
<i>c</i>	0.74	2.15	0	0.0300
Cu(mepyz)(NCO) <sub>2</sub> <sup>b</sup>	0.71	2.02	0	0.0204
<i>c</i>	0.89	2.15	0	0.0947

<sup>a</sup> Estimated error limits:  $g$ ,  $\pm 0.02$ ; % $P$ , negligible;  $-J$ ,  $\pm 0.04$  cm<sup>-1</sup> for Cu(py<sub>2</sub>z)(NCO)<sub>2</sub> and Cu(mepyz)(NCO)<sub>2</sub> and  $\pm 1.5$  cm<sup>-1</sup> for Cu(pd<sub>2</sub>z)(NCO)<sub>2</sub>. <sup>b</sup>  $J$  and  $g$  varied. % $P$  set at zero. <sup>c</sup> Only  $J$  varied. % $P$  set at zero, and  $g$  set to  $g_0$  determined by EPR. <sup>d</sup>  $J$  and % $P$  varied.  $g$  set to  $g_0$  determined by EPR.

For Cu(py<sub>2</sub>z)(NCO)<sub>2</sub>, excellent fits were obtained for both models, and in addition, the fits obtained by allowing both  $J$  and  $g$  to vary generated a  $g$  value of 2.12, in good agreement with the value of 2.15 determined by EPR spectroscopy (Table V). As we have observed previously,<sup>21,40</sup> in cases where the exchange is as weak as that observed here, it is not possible to determine with certainty whether the exchange is one-dimensional or two-dimensional on the basis of the quality of fit to these two models. Nonetheless, we note that better agreement between experiment and theory, as judged by the value of  $F$ , is obtained using the one-dimensional model, suggesting exchange in one dimension is at least dominant. Moreover, in view of the probable unsymmetrical nature of the cyanate bridges in this compound and the fact that >NCO bridges have been considered to provide pathways for ferromagnetic rather than antiferromagnetic exchange,<sup>1</sup> we conclude that the one-dimensional exchange in this complex occurs via the bridging pyrazine ligands. The exchange coupling constant obtained for Cu(py<sub>2</sub>z)(NCO)<sub>2</sub> ( $J = -1.2$  cm<sup>-1</sup>) can be compared with the values reported previously for related complexes which exhibit one-dimensional exchange via bridging pyrazine ligands. The values for Cu(py<sub>2</sub>z)(NO<sub>3</sub>)<sub>2</sub> ( $J = -3.7$  cm<sup>-1</sup>)<sup>41</sup> and Cu(py<sub>2</sub>z)(CF<sub>3</sub>SO<sub>3</sub>)<sub>2</sub> ( $J = -3.8$  cm<sup>-1</sup>)<sup>40</sup> are significantly larger, suggesting that there may be a direct correlation between the strength of exchange and the basicity of the counteranion. The more weakly basic NO<sub>3</sub><sup>-</sup> and CF<sub>3</sub>SO<sub>3</sub><sup>-</sup> anions may interact more weakly with the copper, thus promoting stronger bonds between copper and pyrazine and greater exchange coupling. The thiocyanate complex Cu(py<sub>2</sub>z)(NCS)<sub>2</sub> has been reported to be polymeric and to contain N-bonded thiocyanate groups,<sup>42</sup> and therefore, it may have a structure analogous to that of the cyanate complex described here. The magnetic properties of the thiocyanate compound were not, however, investigated in the earlier work.

Analysis of the magnetic susceptibility data for Cu(mepyz)(NCO)<sub>2</sub> using both the one- and two-dimensional models gave good fits when both  $J$  and  $g$  were allowed to vary. However, the  $g$  values thus obtained are unrealistically low ( $g = 2.02$ ) and significantly below the value determined by EPR spectroscopy ( $g = 2.15$ ). Not unexpectedly, attempts to analyze the data employing the EPR-determined  $g$  value and allowing only  $J$  to vary generated poor fits (Table V). As discussed above, the structure of this compound, compared to that of the pyrazine analogue, may involve less symmetrically bridging neutral ligands and more symmetrically bridging cyanates. This could result in a situation, unlike that of the pyrazine analogue, where the exchange process is complex and does not approximate either simple one-dimensional or two-dimensional behavior. While the

values of  $J$  given in Table V for this compound may provide a rough measure of the strength of the overall exchange, their similarities to corresponding values for the pyrazine analogue are likely fortuitous.

Cu(pd<sub>2</sub>z)(NCO)<sub>2</sub> has a strongly temperature-dependent magnetic moment, indicating the presence of relatively strong antiferromagnetic coupling. This is confirmed by the plot of magnetic susceptibility versus temperature, which shows a broad maximum around 65 K (Figure 3). An increase in susceptibility at the lowest temperatures of the type seen here is often observed in strongly antiferromagnetically coupled copper(II) complexes and has been accounted for by the presence of small amounts of paramagnetic structural impurities.<sup>43</sup> In accordance with the proposed structure for Cu(pd<sub>2</sub>z)(NCO)<sub>2</sub>, its susceptibility data were analyzed according to the one-dimensional isotropic Heisenberg model for  $S = 1/2$  described above with allowance for paramagnetic impurity,  $P$ .<sup>44</sup> Experiment and theory are compared in Figure 3, and the best fit values of the magnetic parameters are given in Table V. A good fit was obtained by treating  $J$  and  $P$  as the adjustable parameters, with  $g$  set equal to the value obtained experimentally by EPR spectroscopy.

In the structure proposed for Cu(pd<sub>2</sub>z)(NCO)<sub>2</sub>, the copper ions are linked by bridging pyridazine ligands and the cyanates are either unsymmetrically bridging (as depicted in Figure 5) or terminal (as found in the analogous Cu(pd<sub>2</sub>z)Cl<sub>2</sub> complex<sup>35</sup>). Whichever form of cyanate coordination is involved, there is no continuous bonding pathway involving short Cu-NCO bonds linking the copper centers, leading to the conclusion that the pathway for exchange is primarily that provided by the pyridazine ligand. This conclusion is supported by the observation that the magnitude of exchange in the cyanate complex ( $J = -44$  cm<sup>-1</sup>) is comparable to that reported for Cu(pd<sub>2</sub>z)Cl<sub>2</sub> ( $J = -35.8$  cm<sup>-1</sup>) and Cu(pd<sub>2</sub>z)Br<sub>2</sub> ( $J = -31.7$  cm<sup>-1</sup>).<sup>45</sup> The chloride complex has been shown by X-ray diffraction to have a chain structure involving just pyridazine bridges.<sup>35</sup> The magnitude of exchange in these pyridazine complexes is significantly greater than that observed in analogous pyrazine-bridged complexes, including those studied in the present work. The largest  $|J|$  so far obtained for pyrazine-bridged copper(II) polymers is that of Cu(py<sub>2</sub>z)Br<sub>2</sub>:<sup>46</sup>  $J = -16.8$  cm<sup>-1</sup>. Pyridazine, which provides a shorter, two-atom bridge, would appear to provide a more facile pathway for magnetic exchange in copper(II) systems than does pyrazine.

**Acknowledgment.** Financial support from the Natural Sciences and Engineering Research Council of Canada is gratefully acknowledged.

**Supplementary Material Available:** Tables of magnetic susceptibility and magnetic moment data and X-ray powder diffraction data ( $2\theta$ ,  $d$ , and  $J$ ) for Cu(py<sub>2</sub>z)(NCO)<sub>2</sub>, Ni(py<sub>2</sub>z)(NCO)<sub>2</sub>, Cu(mepyz)(NCO)<sub>2</sub>, and Cu(pd<sub>2</sub>z)(NCO)<sub>2</sub> and listings of detailed crystallographic data, hydrogen atom coordinates, complete bond lengths and angles including hydrogen atom parameters, anisotropic thermal parameters, torsion angles, intermolecular contacts, and least-squares planes for Cu(mepyz)<sub>2</sub>(NCO)<sub>2</sub> (26 pages). Ordering information is given on any current masthead page.

(40) Haynes, J. S.; Rettig, S. J.; Sams, J. R.; Trotter, J.; Thompson, R. C. *Inorg. Chem.* **1988**, *27*, 1237.

(41) Richardson, H. W.; Hatfield, W. E. *J. Am. Chem. Soc.* **1976**, *98*, 835.

(42) Toeniskoetter, R. H.; Solomon, S. *Inorg. Chem.* **1968**, *7*, 617.

(43) Kobayashi, H.; Haseda, T.; Kanda, E.; Kanda, S. *J. Phys. Soc. Jpn.* **1963**, *18*, 349.

(44) To allow for paramagnetic impurity, the calculated susceptibility,  $\chi_{\text{calc}}$ , is obtained by combining the theoretical susceptibility for the Heisenberg chain model,  $\chi_{\text{chain}}$ , with the Weiss term,  $\chi_{\text{para}} = Ng^2\mu_B^2S(S+1)/3kT$ , in the following way:

$$\chi_{\text{calc}} = (1 - P)\chi_{\text{chain}} + P\chi_{\text{para}}$$

(45) Emori, S.; Inoue, M.; Kubo, M. *Bull. Chem. Soc. Jpn.* **1972**, *45*, 2259.

(46) Inoue, M.; Kubo, M. *Coord. Chem. Rev.* **1976**, *21*, 1.